Light microscopic description of the effects of laser phototherapy on bone defects grafted with mineral trioxide aggregate, bone morphogenetic proteins, and guided bone regeneration in a rodent model

Antonio L. B. Pinheiro,[1,2,3] Luiz G. P. Soares,[1] Gilberth T. S. Aciole,[1] Neandder A. Correia,[1] Artur F. S. Barbosa,[1] Luciana M. P. Ramalho,[1,3] Jean N. dos Santos[3,4]

[1]Center of Biophotonics, School of Dentistry, Federal University of Bahia, Salvador, BA 40110-150, Brazil
[2]Institute of Biomedical Engineering, Camilo Castelo Branco University, São José dos Campos, SP 12245-230, Brazil
[3]National Institute of Optics and Photonics, Physics Institute, University of São Carlos, São Carlos, SP 13560-970, Brazil
[4]Laboratory of Surgical Pathology, School of Dentistry, Federal University of Bahia, Salvador, BA 40110-150, Brazil

Received 25 November 2010; accepted 21 February 2011
Published online 4 May 2011 in Wiley Online Library (wileyonlinelibrary.com). DOI: 10.1002/jbm.a.33107

Abstract: We carried out a histological analysis on bone defects grafted with mineral trioxide aggregate (MTA) treated or not with laser, bone morphogenetic protein (BMP), and guided bone regeneration (GBR). Benefits of the use of MTA, laser, BMPs, and GBR on bone repair are well known, but there is no report on their association with laser light. Ninety rats were divided into 10 groups each subdivided into 3. Defects on G II and I were filled with the blood clot. G II was further irradiated with LED. G III and IV were filled with MTA; G IV was further irradiated with laser. G V and VI, the defects filled with MTA and covered with a membrane (GBR). G VI was further irradiated with laser. G VII and VIII, BMPs were added to the MTA and group VIII further irradiated with laser. G IX and X, the MTA + BMP graft was covered with a membrane (GBR). G X was further irradiated with laser. Laser light ($\lambda = 850$ nm, 150 mW, 4 J/cm^2) was applied over the defect at 48-h intervals and repeated for 15 days. Specimens were processed, cut and stained with H&E and Sirius red and underwent histological analysis. Subjects on group X were irradiated. The results showed different tissue response on all groups during the experimental time. Major changes were seen on irradiated subjects and included marked deposition of new bone in advanced maturation. It is concluded that near infrared laser phototherapy improved the results of the use of the MTA on bone defects. © 2011 Wiley Periodicals, Inc. J Biomed Mater Res Part A: 98A: 212–221, 2011.

Key Words: biomaterial, LLLT, mineral trioxide aggregate

INTRODUCTION

The treatment of bone defects using biomaterials has been extensively studied in the dental field.[1–7] Since the pioneer work by Urist, who demonstrated heterotrophic formation of bone induced by devitalized demineralized bone matrix, a new possibility of treating bone defects was established. Demineralized bone matrix has osteoinductive properties due to the presence of soluble growth factors on its composition.[8] Bone loss may be a result of several pathologies, trauma, or a consequence of surgical procedures. This aspect led to extensive studies on the process of bone repair worldwide. Several techniques for the treatment of bone defects have been proposed, including the use of several types of grafts, membranes, and the association of both techniques.[8]

Mineral trioxide aggregate (MTA) is a powder aggregate, containing mineral oxides that have no cytotoxicity and good biological response. It stimulates tissue repair by increasing cellular adhesion, growth, and proliferation at its surface. The use of MTA has been shown to cause an overgrowth of cementum and on facilitating the regeneration of the periodontal ligament as well as the deposition of new bone.[9–20]

Previous histological reports have indicated that new bone or cementum is formed adjacent to MTA when it is placed in contact with the periodontal tissue or in artificial bone defects.[9–14,21,22] It has antibacterial properties,[23] enhances tissue dissolution, and induces bone formation.[24]

Previous studies suggested that, the rise of pH induced by calcium hydroxide combined with the availability of Ca^{2+} and OH^- ions has a stimulating effect on bone mineralization.[25–28]

Guided bone regeneration (GBR) is a procedure based upon the guided tissue regeneration technique, which is a periodontal surgical procedure, which has been used in the dental clinical practice for more than a decade.[29,30] This procedure is used as a way to stimulate wound healing and to favor the regeneration of tooth supporting structures.[31] Its principles were based upon the selective permeability

Correspondence to: A. L. B. Pinheiro; e-mail: albp@ufba.br
Contract grant sponsors: Conselho Nacional de Desenvolvimento Científico e Tecnológico (CNPq)

provided by the use of membranes on the isolation of tissues, essential for bone repair. Previous studies have demonstrated that such regeneration may occur following this procedure.[29–32] The use GBR associated to the use of biomaterials has been considered to be beneficial for the healing of bones.[8]

Our previous results indicate that near infrared laser phototherapy (NIR LPT) is effective to improve bone repair mainly due to its good penetration on tissues when compared to visible laser light. The use of laser phototherapy (LPT) on studies involving bone healing has been a hot topic lately and many of them have demonstrated positive results, including its association to biomaterials.[33–46]

We have shown that the improvement of bone neoformation and maturation, on irradiated subjects, is associated to the increased deposition of calcium hydroxyapatite (CHA) during early stages of healing. The maturation of the newly formed bone probably represents an increased capacity of secretion by osteoblasts on irradiated subjects. It is well accepted that the deposition of CHA represents bone maturation. Large amounts of CHA on bone are indicative of a more resistant and calcified bone.[33–46]

It is known that LPT has the ability to stimulate cell proliferation, including fibroblasts, which have the capacity to secrete collagen, the main organic component observed during bone repair.[33–46]

Despite the growing successful application of the LPT on bone repair, there are a few studies assessing the association of the laser light with biomaterials.[8,34,36–38,43]

Although several reports have suggested benefits of the isolated or combined use of MTA, BMPs, GBR, and LPT on the repair of bone defects, the associated use of all of these techniques were not studied yet. It might be possible that the observed benefits of the isolated use of each one could be improved with their association.[33–46]

As suggested by previous reports on the current literature, laser light is capable of improving bone healing and may be possible that the use of laser light associated with the MTA may also improve the outcome of the treatment of bone defects.[33–46]

The aim of the present study was to study, histologically, the effect of NIR LPT on the healing of surgical bone defects grafted or not with MTA and associated or not to the use of bone morphogenetic proteins (BMPs) and GBR on a rodent model.

MATERIALS AND METHODS

This study was approved by the Animal Ethics Committee of the Vale do Paraíba University and obeyed national and international guidelines for animal experimentation. Ninety healthy adult male Wistar rats (~2-months-old, average weight 295 ± 25 g) were housed under natural conditions of light, humidity, and temperature at the Animal House of the Research and Development Institute of the Vale do Paraíba University during all experimental period. The sample size was relatively small due to ethical constraints and recommendations of the Ethics Committee. The animals were fed with standard laboratory pelted diet and had water *ad libidum*. The animals were kept in groups of five on individual metallic gages and kept at a day/night light cycle and controlled temperature (22°C) during the experimental period. The animals were randomly distributed into 10 groups and then subdivided into 3 subgroups according to the animal sacrifice timing. The number of experimental groups was determined to allow us to use the MTA under different clinical conditions, such as in association with the technique of GBR, as well as to allow the comparison of the results with similar model used by our team in which other types of biomaterials were used and were reported previously.[8] The distribution of the animals may be seen in Table I.

Prior intramuscular general anesthesia, the animals received 0.04 mL/100 g of atropine subcutaneously. The anesthesia was carried out with 10% Ketamine (Syntec do Brasil, Cotia, SP, Brazil) (0.1 mL/100 g) + 2% Xylazine (Syntec do Brasil) (0.1 mL/100 g). The animals had the right leg shaved and a 3-cm-long incision was performed at the right tibia with a no. 15 scalpel blade. Skin and subcutaneous tissues were dissected down to the periosteum, which was gently sectioned exposing the bone and a 2-mm partial thickness round bone defect was surgically produced (low speed drill, 1200 rpm, under refrigeration) in each animal.

The bone defects on groups II and I were filled only with the blood clot. Bone defects on group II were further irradiated with laser light. The bone defects on the remaining groups were filled with MTA (Angelus®—Angelus Indústria de Produtos Odontológicos S/A, Londrina, PR, Brazil) (III); bone defects of group IV were further irradiated with laser light. On groups V and VI, the bone defects were filled with the MTA and covered with a reabsorbable membrane (Genderm®, Baumer S.A, Mogi das Cruzes, São Paulo, Brazil). Bone defects of group VI were further irradiated with laser light. On groups VII and VIII, a *pool* of BMPs (Genpro®, Baumer S.A. Mogi das Cruzes, São Paulo, Brazil) was added to the biomaterial (MTA); group VII was further irradiated with laser light. On groups IX and X, the MTA + BMP graft was covered with the membrane (GBR). Bone defects on group X were further irradiated with laser light. All wounds were routinely sutured and the animals received a single dose of Pentabiotico® (Penicillin, Streptomycin, 20,000 UI, Fort Dodge Ltda, Campinas, SP, Brazil) (0.02 mL/100 g) immediately after surgery. Animal death

TABLE I. Distribution of the Experimental Groups

Group	Subgroups	*n*	Protocol
I	I15/I21/I30	9	Control (Clot)
II	II15/II21/II30	9	NIR LPT
III	III15/III21/III30	9	MTA
IV	IV15/IV21/IV30	9	MTA + NIR LPT
V	V15/V21/V30	9	MTA + GBR
VI	VI15/VI21/VI30	9	MTA + GRB + NIR LPT
VII	VII15/VII21/VII30	9	MTA + BMP
VIII	VIII15/VIII21/VIII30	9	MTA + BMP + NIR LPT
IX	IX15/IX21/IX30	9	MTA + BMP + GBR
X	X15/X21/X30	9	MTA + BMP + GBR + NIR LPT

TABLE II. Semiquantitative Criteria Used for the Light Microscopy Analysis

Score Criterion	Discrete	Moderate	Intense
Bone reabsorption	Presence of <25% of the reabsorption of the graft remnants and/or the surgical bed.	Presence of 25–50% of the reabsorption of the graft remnants and/or the surgical bed.	Presence of >75% of the reabsorption of the graft remnants and/or the surgical bed.
Bone neoformation	Presence of <25% of newly formed bone similar to adjacent untreated bone tissue.	Presence of 25–50% of newly formed bone similar to adjacent untreated bone tissue.	Presence of >50% of newly formed bone similar to adjacent untreated bone tissue.
Inflammatory infiltrate	Presence of <25% of inflammatory cells in the area.	Presence of 25–50% of inflammatory cells in the area.	Presence of >50% of inflammatory cells in the area.
Collagen deposition	Presence of <25% of collagen deposition in the area.	Presence of 25–50% of collagen deposition in the area.	Presence of >50% of collagen deposition in the area.

occurred after 15, 21, and 30 days after the surgery with an overdose of general anesthetics.

NIR LPTP was carried out with the Twin Laser® device (MMOptics, São Carlos, São Paulo, Brazil; $\lambda = 850$ nm, 150 mW, $\phi = 0.5$ cm^2, 4 J/cm^2) and was transcutaneously applied on four points around the bone defect at 48-h intervals (4 J/cm^2, per point) being the first session carried out immediately after surgery and repeated at every 48 h during 15 days (16 J/cm^2 per session) and a total treatment dose of 112 J/cm^2. Doses used in this study were based upon previous studies carried out by our group.[8]

Following animal death, the samples were longitudinally cut under refrigeration (Bueler®, Isomet TM1000; Markham, Ontario, Canada) and the specimens kept in 10% formalin solution for 24 h. The specimens were routinely processed to wax, cut, and stained with Hematoxylin and Eosin and Sirius red and underwent histological analysis[8,34,36–38,42] (Table II) at the Laboratory of Surgical Pathology of the School of Dentistry of the Federal University of Bahia by a experienced pathologist in a blind manner using a Light microscope (AxioStar®, Zeiss, Germany).

RESULTS

Clot

On day 15, the bone defect was partially filled with newly formed bone displaying nonaligned osteocytes as well as the presence of thin and irregular trabeculi. Medullar tissue and chronic inflammation were seen and scored as discrete. Osteoblastic activity could be seen and there were no signs of bone reabsorption. On day 21, the bone defect was mostly filled with new bone that was more regular than that type of bone seen on the 15th day. Discrete chronic inflammation was observed at this stage. Some specimens of this group showed remnants of cartilaginous tissue, and no signs of bone reabsorption were seen [Fig. 1(A)]. At the end of the experimental period, the bone defect was completely filled by lamellar bone and few Haversian systems were seen. Bone trabeculi were present and were more regularly disposed. The trabeculi showed some osteocytes as well as remnants of cartilage surrounded by bone. Neither reabsorption nor inflammation was observed at this time.

MTA

On day 15, the bone defect was mostly filled by neoformed bone that was characterized by the presence of interconnecting trabeculi containing osteocytes on its matrix and osteoblasts at their surface. Remnants of cartilage and chronic inflammation were also seen dispersed within a fibrovascular tissue. A few points of surface necrosis and remnants of the biomaterial could be seen at this time [Fig. 1(B)]. Bone reabsorption was observed at this stage. On day 21, a regular neoformed bone dispersed in few medullar spaces covered the bone defect and discrete chronic inflammation was observed. The new bone showed osteocytes as well as basophilic reversal lines, and osteoblasts were seen at the osseous surface. At the end of the experimental time, the bone defect was filled by bone without signs of inflammation. Small bone trabeculi, medullar tissue, surface necrosis, and remnants of the biomaterial were also seen at this time.

MTA + GBR

On day 15, interconnecting bone trabeculi showing nonaligned osteocytes as well as active osteoblasts at the periphery of the trabeculi filled the bone defect. In a few cases, delicate bone fragments, usually immature, were seen within a highly vascularized medullar tissue. In some specimens, surface necrosis could be seen. Beneath the necrosis, a band of fibrous connective tissue was detected as well as chronic inflammatory infiltrate and remnants of the biomaterial. On day 21, the bone defect was filled by thick newly formed bone usually showing interconnecting bone trabeculi, nonaligned osteocytes, and basophilic reversal lines. Areas of superficial necrosis were also observed in some specimens as well as the presence of remnants of the biomaterial. At the end of the experimental time, the bone defect was filled by new bone that was characterized by few medullar spaces and irregular small bone fragments. In few specimens, remnants of cartilage could be seen as well as tissue necrosis extending down to the medulla. Remnants of the biomaterial were also seen at this stage [Fig. 1(C)].

MTA + BMP

On day 15, the bone defect was filled by interconnecting bone trabeculi, few medullary spaces, nonaligned osteocytes,

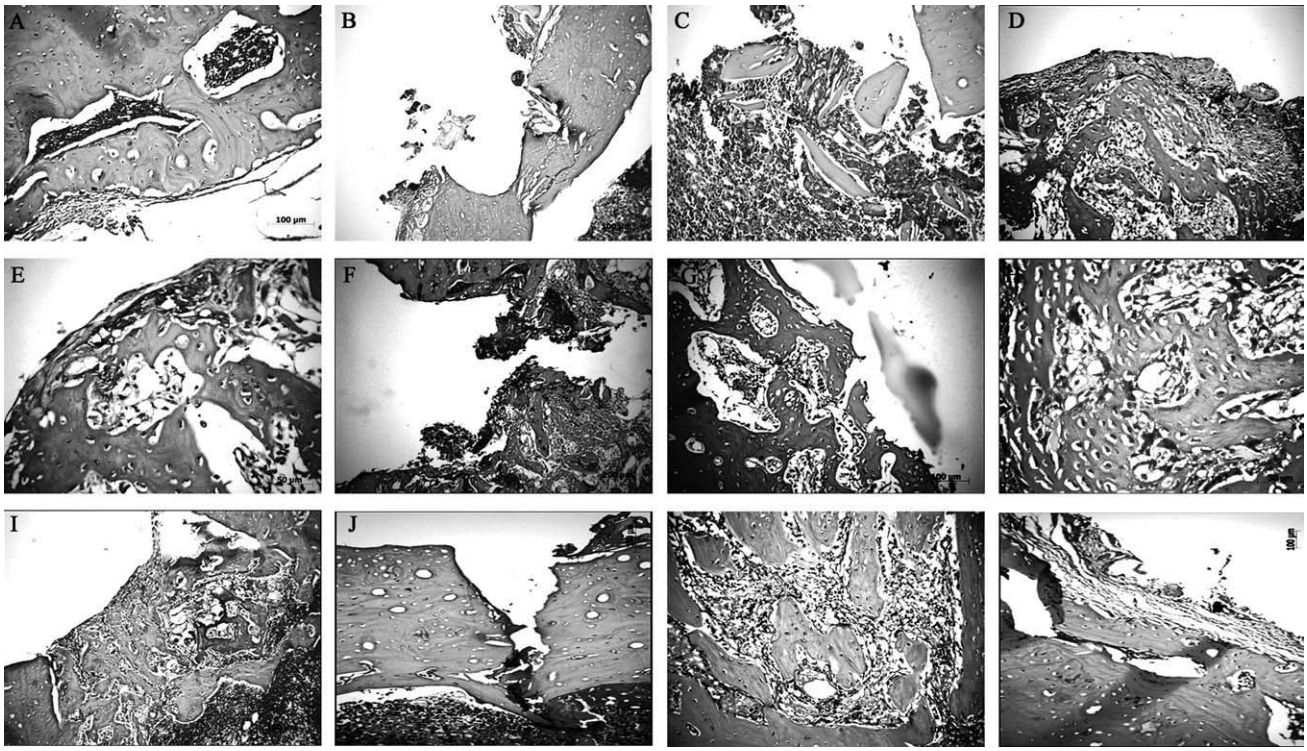

FIGURE 1. (A) Photomicrography of a control specimen on day 21 showing the bone defect completely filled with newly formed extending down to the medullar tissue and displaying osteocytes nonaligned and basophilic reversal lines. (B) Photomicrography of a specimen grafted with MTA on day 15 showing the bone spicules amidst bone defect whose superficial area shows bone necrosis. Note inferior margin with bone walls close to medullar tissue. (C) Photomicrography of a specimen of the MTA + GBR group on day 21 showing the bone defect filled by bone spicules of variable size amidst inflammation composed of lymphocytes and macrophages. Note necrosis due to the biomaterial on surface. (D) Photomicrography of specimen of the group MTA + BMP on day 15 showing the fibrous band with small areas of necrosis and remnant of the biomaterial (seen on top right), followed by the bone defect filled by newly formed bone in the form of interconnecting that displays osteocytes nonaligned. There were signs of reabsorption. (E) Photomicrography of a specimen of group MTA + BMP + GBR on day 15 showing the bone defect partially filled with bone spicules and trabeculi extending from one cortical side, and the other whose surface displays necrosis, cartilage remnants, and osteocytes nonaligned are also observed. (F) Photomicrography of group NIR LPT on day 15 showing the bone defect filled by interconnecting and newly formed bone with nonaligned osteocytes and discrete basophilic reversal lines, amidst medullar tissue. (G) Photomicrography MTA + NIR LPT on day 15 showing a fibrous band with remnants of the biomaterial and necrosis followed by irregular trabeculi displaying nonaligned osteocytes and some medullar tissue. (H) Photomicrography of specimen of group MTA + NIR LPT on day 21 showing newly formed bone displaying numerous osteocytes and active multinucleated giant cells amidst fibrous tissue with chronic inflammation. (I) Photomicrography of a specimen of group MTA + GBR + NIR LPT on day 15 showing the bone defect filled by interconnecting and newly formed bone and displaying nonaligned osteocytes. No signs of reabsorption were seen, and inferior part showed extensive irregular bone close to medullar tissue. (J) Photomicrography of a specimen of group MTA + BMP + NIR LPT on day 15 showing the bone defect displaying small bone spicules and areas of necrosis. (L) Photomicrography of a specimen of group MTA + BMP + NIR LPT on day 15 showing the bone defect filled by interconnecting trabeculi displaying active osteoblasts, osteocytes nonaligned, and reversal basophilic lines amidst inflamed tissue. Note that neoformation progressed of bone cortical as seen on the bottom. (M) Photomicrography of a specimen of group MTA + GBR + BMP + NIR LPT on day 21 showing a fibrous band with remnants of the biomaterial and necrosis followed by extensive displaying osteocytes nonaligned and some medullar tissue.

and active osteoblasts at the periphery of bone trabeculi. At the surface, a band of fibrous connective tissue and small areas of necrosis could be seen as well as both remnants of the biomaterial and osteoclasts [Fig. 1(D)]. On day 21, the newly formed bone was thick and irregular and showed irregular osteocytes and few medullary spaces. In a few cases, a band of fibrous connective tissue and remnants of the biomaterial covered the surface of the bone defect. These remnants were associated to foreign body reaction, and there were signs of bone reabsorption. At the end of the experimental period, necrotic debris was seen at the surface as well as macrophages and bony fragments were seen extending down to the center of the bone defect. The core of the bone defect showed irregular bone trabeculi and the presence of osteocytes. Discrete chronic inflammation was seen during all experimental period.

MTA + BMP + GBR

On day 15, there was surface necrosis extending down to the core of the bone defect. Irregular bone fragments and few remnants of the biomaterial were seen associated to macrophages. In many cases, an area of necrosis was observed and, beneath it, a band of fibrous tissue was seen. Large number of bony fragments associated to basophilic reversal lines as well as a large amount of remnants of cartilage was noticed [Fig. 1(E)]. Irregular osteoid tissue was also seen at this stage. On day 21, the bone defect was filled by newly formed tissue showing either regular or irregular

deposition. Irregular osteocytes, basophilic reversal lines, and few medullary spaces were also seen. At the surface, besides the presence of remnants of the biomaterial, a band of fibrotic tissue was also seen as well as evidence of bone reabsorption, and moderate chronic inflammation. At the end of the experimental time, the bone defect was partially or completely filled by newly formed bone displaying nonaligned osteocytes and few medullary spaces. In some cases, at the surface, a band of fibrous tissue and remnants of the biomaterial were seen. No inflammation was observed at this stage.

NIR LPT

On day 15, the bone defect was partially filled by newly formed bone. Interconnecting delicate bone trabeculi, nonaligned osteocytes, and basophilic reversal lines were seen at this time. In some specimens, osteoblasts and remnants of cartilage were seen at the surface [Fig. 1(F)]. The newly formed bone was dispersed on medullar tissue and no signs of reabsorption could be seen. On day 21, the newly formed bone was regularly distributed and showed no signs of reabsorption. At the end of the experimental period, the bone defect was mostly filled by newly formed bone that was either regular or irregularly distributed and showed few medullar spaces. No signs of reabsorption were seen.

MTA + NIR LPT

On day 15, surface necrosis was observed as well as the presence of an irregularly distributed; either thin or thick newly formed interconnecting bone trabeculi, with nonaligned osteocytes and basophilic reversal lines [Fig. 1(G)]. The presence of remnants of the biomaterial was also seen at the surface. There was evidence of sites of reabsorption of the bone. On day 21, the bone filling the bone defect was either thick or thin and also showed nonaligned osteocytes, basophilic reversal lines, and few medullary spaces. No evidence of reabsorption was seen at this stage [Fig. 1(H)]. At the end of the experimental period, the bone defect was filled by newly formed bone and focal area displaying reabsorption was seen. Chronic inflammation was seen during all experimental time.

MTA + GBR + NIR LPT

On day 15, the bone defect was either partially or completely filled by irregular bone trabeculi dispersed on medullar tissue. The bone showed nonaligned osteocytes and active osteoblasts at the periphery of bone trabeculi [Fig. 1(I)]. In a few cases, bony fragments were observed. Foci of necrosis could also be seen at the surface at this stage. Remnants of the biomaterial were also seen in all cases as well as a band of fibrotic tissue. These remnants were sometimes observed incorporated to the newly formed bone and they assumed a crystalloid aspect. Despite the presence of some foci of necrosis close to the bony fragments, deeper region (within the bone defect) showed newly formed bone. No evidence of bone reabsorption could be seen at this stage, but chronic inflammation was seen. On day 21, the bone defect was mostly filled with interconnecting bone trabeculi, displaying nonaligned osteocytes and basophilic reversal lines as well as discrete chronic inflammation. No signs of necrosis or reabsorption could be seen at this stage. A delicate mesh of newly formed bone and medullary tissue filled the bone defect. In some cases, a band of connective tissue was also seen at surface. No inflammation was found at this time.

MTA + BMP + NIR LPT

On day 15, the bone defect was partially covered by necrotic tissue and showed foci of remnants of the biomaterial [Fig. 1(J)]. Beneath it, bony fragments dispersed within necrotic tissue were seen. In some cases, the newly formed bone was thick and showed osteocytes and few medullary spaces. The inferior margin of the bone defect showed a thin bone wall [Fig. 1(L)]. On day 21 thick newly formed bone, containing remnants of the biomaterial filled the bone defect. In some specimens, a band of fibrosis was present and usually it projected itself within the medulla. At the end of the experimental period, the bone defect was completely filled by a dense newly formed bone sometimes irregular, osteocytes, and basophilic reversal lines. Discrete chronic inflammation was seen during all times.

MTA + GBR + BMP + NIR LPT

On day 15, the bone defect was filled by newly formed bone that was distributed in an irregular manner and showed both osteocytes and remnants of the biomaterial within it. Some specimens showed osteoblasts at the surface and signs of bone reabsorption at this time. On day 21, the histological aspect varied: one specimen showed remnants of the biomaterial dispersed on granulation tissue, lamellar

TABLE III. Summary of the Histological Analysis

Criterion/Group	Bone Reabsorption	Bone Neoformation	Inflammatory Infiltrate	Collagen Deposition
Clot	Absent	Intense	Discrete (chronic)	Moderate
MTA	Absent	Moderate	Discrete (chronic)	Moderate
MTA + GBR	Discrete	Moderate	Discrete (chronic)	Moderate
MTA + BMP	Moderate	Moderate	Absent	Moderate
MTA + BMP + GBR	Discrete	Intense	Moderate (chronic)	Moderate
NIR LPT	Absent	Intense	Absent	Intense
MTA + NIR LPT	Discrete	Intense	Absent	Intense
MTA + GBR + NIR LPT	Absent	Intense	Moderate (chronic)	Intense
MTA + GBR + BMP + NIR LPT	Discrete	Intense	Discrete	Intense

bone, and remnants of cartilage [Fig. 1(M)]; one specimen showed newly formed bone and osteocytes. Others showed newly formed bone, of variable thickness projecting from the borders of the bone defect, displaying osteocytes, basophilic reversal lines, and remnants of the biomaterial. The bone defect was filled by newly formed bone containing osteocytes, basophilic reversal lines, and remnants of both cartilage and the biomaterial. Discrete chronic inflammation was seen throughout the experimental time. A summary of the results may be seen in Table III.

DISCUSSION

Natural processes of healing should be allowed to take their usual course, and any interference on them should be attempted only when there is a demonstrable need or substantial advantage for the patient. Bone healing has been under extensive investigation for many years.

The Wistar rat experimental model used in this study possesses advantages such as allowing a rapid healing period, animals easily lodged and fed, resistance to climatic variations, low cost, besides being routinely used in other experimental conditions involving bone reconstruction.[47]

Critical size defects (CSDs) do not repair well because it exceeds the body's ability to regenerate adequate amounts of bone fast enough. This lesion is defined as a defect that heals by less than 10% bony regeneration during the lifetime of the individual. The CSDs in the long bones of rats have not been as well studied as those in the calvaria. However, the creation of a CSD may still be used if long bones are needed to test.[48]

The CSD, as an experimental model, was originally developed as a model of fibrous nonunion and was intended to standardize the testing of bone repair materials that could be used as alternatives to bone allografting or autografting, and was originally defined as "the smallest size intraosseous defect in a particular bone and species of animal that will not heal spontaneously during the lifetime of the animal" by Schmitz and Hollinger in 1986. The critical size tibia defect in rats was then defined as 1-mm round defect and, by definition, it is supposed to be unable to heal spontaneously.[48]

In the present study, we opted to use a larger bone defect than a critical size one intending to increase the severity of the damage to the bone. It is important to note that similar model has been in use by our group for more than a decade, and its effectiveness well reported elsewhere in the literature.[8,31–33,35,40–42,44,47] The development of nonunions occurs only in fractures. It is characterized by the deposition of fibrous tissue instead of bone. Despite bone formation may occurs eventually, the restoration of the morphology and function are impaired. On the present study, we were unable to find any such phenomena as we created a partial thickness surgical defect and not a fracture.

Over the past years, our group has been working extensively on the study of the effects of the use of NIR LPT on bone using different animal models. In these studies, we have also used many assessment methods to determine the effects of the NIR LPT on bone including the use of histology,[33–37,40,42–44] computadorized morphometry,[46] SEM,[39,45] and Raman spectroscopy.[38,39,41,47]

In all previously used protocols, models and parameters, we were able to demonstrate that NIR LPT caused important tissue responses during healing and these were responsible for a quicker repair process as well as on the improved quality of the newly formed bone.[8,33–47]

We have found that the advanced bone maturation, as observed in irradiated subjects, shall be due to an increased deposition of CHA.[38,39,41,47] The maturation represents the improved ability of more mature osteoblasts to secrete CHA in irradiated subjects. Deposition of CHA represents bone maturation, and increased amount of CHA on the bone is indicative of a more resistant and calcified bone.[8,33–39,42–44,47]

It is known that LPT, at specific wavelengths, has the capability to stimulate cell proliferation, including fibroblasts, which are major secretors of collagen, an important organic component present during bone repair.[8] It is important to consider that the presence of fibroblasts and increased secretion of collagen found in the present study mean that there was a ongoing bone repair and not the development of fibrous nonunion.

It is known that LPT stimulates cell proliferation, including fibroblasts; this cell has the capacity to secrete collagen. In the bone matrix, hydroxyapatite crystals have been observed, and they will grow in clusters, which later coalesce to completely calcify the matrix, filling the spaces between and within the collagen fibers. It is known that, during the many stages in bone healing, several cytokines and growth factors regulate matrix production. Various factors such as BMPs, TGFβ, and PDGF have been successfully used to augment healing in experimental models. LPT also has positive effects on the release of several such mediators.[33–46]

MTA is a white or gray powder containing calcium oxide 65%, calcium silicate 21%, ferric oxide 5%, calcium aluminate 4%, calcium sulfates 2.5%, magnesium oxide 2%, sodium, and potassium oxide 0.5%. Its pH (12.5), both biologically and histologically, makes it similar to calcium hydroxide. Hydration of the powder results in a colloidal gel that solidifies to a hard structure. Unlike other cements, which demand a completely dry field, MTA is indicated when moisture control is inadequate, without loss of its properties and it is not reabsorbable. MTA is less toxic and has a powerful bacteriostatic effect with lower marginal percolation. Because of its hydrophilic properties and setting in a moisture environment, perfect isolation is counter indicated. The setting time for the cement is nearly 4 h. Because of the slow setting time, the initial looseness of the MTA after mixing can make the material difficult to handle. In this study, the MTA was handled and inserted quickly into the bone defect. When the MTA mixture was dry, it become crumbly and unmanageable.[47]

MTA is a powder aggregate containing mineral oxides. Besides its noncytotoxicity and good biological action, it stimulates tissue repair because of cellular adhesion, growth, and proliferation on its surface. MTA has been shown to result in the overgrowth of cementum and in

facilitating regeneration of the periodontal ligament and formation of bone.

As far as we are concerned this is the first histological report to describe, histologically, the mechanisms of the repair bone defects treated or not with laser light, MTA, BMPs, and GBR. The comparison of our results with other previous reports is difficult. This is the first report of the use of this model. Our previous experience using other types of biomaterials already reported in the literature is also suggestive that the association of NIR LPT with biomaterials causes improvement on the repair of bone defects.[8]

A previous report from our team evaluated the effect laser light associated to MTA on the alveolar bone repair process. We found that laser-irradiated sockets substantial formation of thick interwoven osteocyte-rich trabecular bone, with an evident osteoblastic rimming when compared to the use of MTA as well as to untreated controls showing that laser light was the most successful treatment to improve alveolar bone repair.[49]

This study was designed to carry out a qualitative assessment of the repair process, as this is the first report of its kind and the description of the process considered an appropriated method of assessing the effects of different techniques used both isolated or in combination, allowing us to have a qualitative "picture" of the process.

The present study is the histological analysis of the study recently published by our team in which Raman spectroscopy was used as assessment method and showed results aligned with the histological findings of the present study.[47] This aspect is important, as the only use of histological findings could be considered inadequate by anyone and some authors suggested that this kind of data would be better utilized if correlated with other test such as radiological evaluation or with mechanical tests of the bone.[50–52]

In the Raman study we found that, laser-irradiated subjects, showed significant higher levels of CHA in the earlier period of healing. However, these levels were similar to the observed when the association of MTA + BMP + GBR + Laser was used. Lowest levels of deposition were observed when MTA + Laser and MTA + GBR were used. At the end of the experimental period, all defects were found to be similar. However, higher levels of CHA were seen in group MTA + GBR + Laser and lower in group MTA + Laser. As increased peaks of CHA are indicative of bone maturation, the association of MTA, GBR, and laser resulted in a more advanced repair.[47]

We found differences among the groups during all experimental timing. It is important to keep in mind that the MTA probably acted as a local irritant even on being considered biocompatible. When the MTA was associated to GBR, no major morphological changes were seen. But, we observed crystalloid structures that may be attributable to the MTA as its anhydrous phases involve the formation of crystals, an important physiologic event in the formation of the bone.[53] Again, these changes might be attributed to the presence of the MTA. The addition of BMPs to the MTA did not improve the process significantly. When the MTA + BMP graft was associated to GBR, the major observed change was of irregular osteoid tissue, whose appearance may be attributed to the GBR technique. The use of NIR LPT caused both early deposition of bone trabeculi and the cessation of the osteoclastic activity,[54] which plays a pivotal role on the remodeling of the bone.[55–57] These lines were not seen on controls but were present on LPT and on MTA + BMP + GBR treated subjects. This may be indicative that the use alone of the LPT may cause similar results to the use of the association of conventional techniques alone.

Later on, untreated controls and MTA-grafted subjects showed similar healing pattern as seen at early stages. We also found remnants of cartilaginous tissue on the controls that may be indicative of evolution of the process. The MTA seemed to cause a small delay in the repair process. The use of the GBR caused the presence of thick newly formed bone. Increased thickness might have been caused by the GBR technique. Adding BMPs to the biomaterial also caused the appearance of thick and irregular newly formed bone. However, despite remnants of the graft causing foreign body reaction there was no bone reabsorption. The use of the BMPs might have caused more bone deposition during the repair due to its properties.

The use of the GBR to the association of MTA and BMPs caused no major improvement on the repair. The use of the LPT caused the deposition of a regularly distributed newly formed bone. On the other hand, MTA grafts irradiated caused irregular deposition of bone. The association of the LPT with GBR did not improve the repair significantly. The LPT associated to the MTA, BMPs, and GBR caused variable responses including the presence of newly formed bone, of variable thickness, projecting from the borders of the bone defect. This was not seen on other groups.

At the end of the experimental period, the controls showed the bone defect completely filled by lamellar trabecullar bone and few Haversian systems. The use of GBR or not on MTA-grafted subjects caused a deposition of a less dense bone. The addition of BMPs caused the appearance necrotic debris and macrophages. The use of MTA, BMPs, and GBR caused the presence of newly formed bone either partially or completely filling the bone defects. LPT-treated subjects showed the bone defect mostly filled regular or irregular bone. The use of MTA caused the appearance of newly formed bone of varied thickness. Using NIR LPT on grafts subjected to GBR did not affect the overall repair much. NIR LPT associated to MTA and BMPs caused the complete filling of the bone defect by a dense newly formed bone. The laser light associated to MTA, BMPs, and GBR also resulted in the deposition of newly formed bone and remnants of cartilage. It is possible that the chondrogenic differentiation occurred due to mesenchymal stem cells present in the bone marrow, and represents the presence of progenitor cells capable of differentiating into osteoblasts. Thus, these cartilage remnants could play a key role as scaffold in the bone repair.

One may question that it is expected inflammatory response to develop against bone repair materials (i.e., scaffold) as these materials, no matter how biocompatible they are, they are foreign materials. In the present study we

found more inflammatory response in clot group, in which there is no scaffold applied at all, than the ones in MTA + BMP, NIR LPT, and MTA + NIR LPT groups. This may be explained by previous investigations that have indicated that, the persistence of the inflammatory response in the later phases of alveolar bone repair might be a result of a phlogistic activity of residual blood clots.[49,58]

In terms of bone neoformation, we found more bone formation in clot group than on the ones in MTA (in which there is osteoconductive scaffold), MTA + GBR (in which there is osteoconductive scaffold and GBR was induced), and MTA + BMP (in which there is osteoconductive scaffold and osteoinductive cytokine). Despite the presence of MTA to be expected to facilitate the process of bone deposition, due to its biochemical properties, such as alkalinity and high content of calcium phosphate, calcium oxide and silica, which are important inorganic constituents widely required for bone mineralization, this material probably, due to some phlogistic activity promoted by its handling during the filling of the defect, delayed the process. It may be speculated that MTA handling within the alveolar wound caused a disarrangement of part of the blood clot and altered the bone regeneration process.[49]

We were not able to find in the literature any previous reports on the association of MTA with BMPs. Despite we have shown that the use of BMPs may improve the outcome of bone healing when associated with LPT, in the present study it was not the case. This was probably due to the properties of the MTA.

It has also been demonstrated by our group that, the use of GBR, is helpful in the healing of bone defects and that the association with LPT improves the outcome of this therapeutic approach as demonstrated previously by our using different models.[33–47]

The results of our study indicate that irradiated bone showed increased osteoblastic proliferation, collagen deposition, and bone neoformation when compared to nonirradiated one. The results of our studies and others indicate that bone irradiated mostly with IR wavelengths shows increased osteoblastic proliferation, collagen deposition, and bone neoformation when compared to nonirradiated bone. The effects observed in irradiated subjects might be a result of positive effects of laser irradiation on the cell membrane and mitochondria. Laser light influences the production of ATP and it is more effective at when used at early stages and depends on the physiologic status of the cell.[33–47]

Vascularization is also an important and decisive factor for the healing of wounds and it is improved after the use of laser light as well as increased release of mediators such as PGE_2 that is also increased after irradiation. There is evidence that PGE_2 is also produced by osteoblasts and that its effects may be therapeutic or adverse.[33–46]

It is known that laser light stimulates cell proliferation, including fibroblasts; this cell has the capacity to secrete collagen. In the bone matrix, hydroxyapatite crystals have been observed, and they will grow in clusters, which later coalesce to completely calcify the matrix, filling the spaces between and within the collagen fibers. It is known that, during the many stages in bone healing, several cytokines and growth factors regulate matrix production.[33–46]

Various factors such as BMPs, transforming growth factor-β, and platelet-derived growth factor have been successfully used to augment healing in experimental models. Laser light also has positive effects on the release of several such mediators.[33–46]

A parameter able to produce any photo biological response alone does not exist. The photoresponse depends on the conjugation of different parameters. It still remains uncertain if bone stimulation by laser light is a general effect or if the isolate stimulation of osteoblasts is possible. It is possible that laser's effect on bone regeneration depends not only on the total dose of irradiation, but also on the irradiation time and the irradiation mode. Most importantly, the threshold parameter energy density and intensity are biologically independent of one another. This independence accounts for the success and the failure of the treatment.[33–46]

One may question the advantage of using an *in vitro* experiment where the direct influence of LPT on osteoblasts and the MTA-scaffold could be analyzed. In the present study, we opted for using an *in vivo* model and not an *in vitro* one as the animal model allowed us a more detailed and "close" to human tissue response analysis of the different treatments carried out as well as the host-responses to them. The host-response on *in vitro* model is very limited or not possible of simulation in many aspects. For instance, despite recent study[59] have found *in vivo* adhesion of osteoblasts to MTA, an *in vitro* report[60] using osteoblasts failed to get cell adhesion to MTA. In the present study, we often observed a close contact of the graft with the bone matrix and possibly inducing the formation of important components for bone neoformation as a result of the interaction of the MTA, the matrix, and the host.[61,62] Then, biological responses may be similarly detected using different assessment methods.

CONCLUSION

The results showed different tissue response on all groups during the experimental time. Major changes were seen in irradiated subjects and included marked deposition of new bone seen in advanced maturation. It is concluded that NIR LPT improved the results of the use of the MTA on bone defects.

REFERENCES

1. Pastori CM, Zorzetto DLG, Toledo Filho JL, Marzola C. Implantes de bioapatita + osseobond® + membrana reabsorvível dentoflex + aglutinante dentoflex. [Implants of bioapatite + osseobond® + dentoflex reabsorbable membrane + dentoflex link agent: Surgical cases report]. Rev Bras Ciênc Estomatol 1996;1:51–63.
2. Reddi AH. Initiation of fracture repair by bone morphogenetic proteins. Clin Orthop Relat 1998;355(Suppl):S66–S72.
3. Park YJ. Enhanced guided bone regeneration by controlled tetracycline release from poly(L-lactide) barrier membranes. J Biomed Mater Res 2000;51:391–397.
4. Segundo T. Avaliação dos Enxertos Ósseos e Homólogos Utilizados em Implántodontia. [Assessment of bone grafts and similar used in implantology]. RGO 2000;48:217–220.

5. Restrepo LL, Marzola C, Consolaro A, Pereira AC, Toledo Filho JL, Andreo JC. Avaliação de implantes de osso bovino liofilizado "Osseobond"® e membrana reabsorvível de osso bovino liofilizado. [Assemment of liophilized bovine bone "Osseobond"® and reabsorbable bovine bone membrane]. Available at http://www.odontologia.com.br/artigos. 02 March 2001.
6. Taga EM, Mulatinho J. Biomateriais para uso em Clínica Médico-Odontológica. [Biomaterials used on medical-dental clinics]. Available at http://www.dentoflex.com.br. 05 February 2001.
7. Nyman S, Lindhe J, Karring T, Rylander H. New attachment following surgical treatment of human periodontal disease. J Clin Periodontol 1982;9:290–296.
8. Pinheiro ALB, Gerbi MEMM. Photoengineering of bone repair processes. Photomed Laser Surg 2006;24:169–178.
9. Torabinejad M, Hong CU, Lee SJ, Monsef M, Pitt Ford TR. Investigation of mineral trioxide aggregate for root end filling in dogs. J Endod 1995;21:603–608.
10. Torabinejad M, Hong CU, Pitt Ford TR. Physical properties of a new root end filling material. J Endod 1995;21:349–353.
11. Torabinejad M, Hong CU, Pitt Ford TR, Kariyawasam SP. Tissue reaction to implanted super-EBA and mineral trioxide aggregate in the mandible of guinea pigs: A preliminary report. J Endod 1995;21:569–571.
12. Torabinejad M, Hong CU, Pitt Ford TR, Kettering JD. Cytotoxicity of four root end filling materials. J Endod 1995;21:489–492.
13. Torabinejad M, Pitt Ford TR, Abedi HR, Kariyawasam SP, Tang HM. Tissue reaction to implanted root-end filling materials in the tibia and mandible of guinea pigs. J Endod 1998;24:468–471.
14. Torabinejad M, Chivian N. Clinical applications of mineral trioxide aggregate. J Endod 1999;25:197–205.
15. Schwartz RS, Mauger M, Clement DJ, Walker WAM. Mineral trioxide aggregate: A new material for endodontics. J Am Dent Assoc 1999;130:967–975.
16. Zhu Q, Haglund R, Safavi KE, Spangberg LSW. Adhesion of human osteoblasts on root-end filling materials. J Endod 2000;26:404–406.
17. Regan JD, Gutmann JL, Witherspoon DE. Comparison of Diaket and MTA when used as rootend filling materials to support regeneration of the periradicular tissues. Int Endod J 2002;35:840–847.
18. Economides N, Pantelidou O, Kokkas A, Tziafas D. Short-term periradicular tissue response to mineral trioxide aggregate (MTA) as root-end filling material. Int Endod J 2003;36:44–48.
19. Al-Rabeah E, Perinpanayagam H, MacFarland D. Human alveolar bone cells interact with ProRoot and tooth-colored MTA. J Endod 2006;32:872–875.
20. Oviir T, Pagoria Ibarra G, Geurtsen W. Effects of gray and white mineral trioxide aggregate on the proliferation of oral keratinocytes and cementoblasts. J Endod 2006;32:210–213.
21. Holland R, de Souza V, Nery MJ, Otoboni Filho A, Barnabé PFE, Dezan E Jr. Reaction of dog's teeth to root canal filling with mineral trioxide aggregate or a glass ionomer sealer. J Endod 1999;25:728–730.
22. Moretton TR, Brown CE Jr, Legan JJ, Kafrawy AH. Tissue reactions after subcutaneous and intraosseous implantation of mineral trioxide aggregate and ethoxybenzoic acid cement. J Biomed Mater Res 2000;52:528–533.
23. Bystrom A, Claesson R, Sundqvist G. The antibacterial effect of camphorated paramonochlorophenol, camphorated phenol and calcium hydroxide in the treatment of infected root canals. Endod Dent Traumatol 1995;1:170–175.
24. Mitchell PJ, Pitt Ford TR, Torabinejad M, McDonald F. Osteoblast biocompatibility of mineral trioxide aggregate. Biomaterials 1999;20:167–173.
25. Tronstad L, Andreasen JO, Hasselgren G, Kristerson L, Riis I. pH changes in dental tissues after root canal filling with calcium hydroxide. J Endod 1980;7:17–21.
26. De Moor RJ, DeWitte AM. Periapical lesions accidentally filled with calcium hydroxide. Int Endod J 2002;35:946–958.
27. De Rossi A, Silva LA, Leonardo MR, Rocha LB, Rossi MA. Effect of rotary or manual instrumentation, with or without a calcium hydroxide/1% chlorhexidine intracanal dressing, on the healing of experimentally induced chronic periapical lesions. Oral Surg Oral Med Oral Pathol Oral Radiol Endod 2005;99:628–636.
28. Tronstad L. Root resorption-etiology, terminology and clinical manifestations. Endod Dent Traumatol 1988;4:241–252.
29. Gottlow J, Nyman S, Karring T, Lindhe J. New attachment formation as the result of controlled tissue regeneration. J Clin Periodontol 1984;11:494–503.
30. Garrett S. Periodontal regeneration around natural teeth. Ann Periodontol 1996;1:621–666.
31. Stahl SS, Froum S, Tarnow D. Human histologic responses to guided tissue regenerative techniques in intrabony lesions. Case reports on 9 sites. J Clin Periodontol 1990;17:191–198.
32. Cortellini P, Clauser C, Prato GP. Histologic assessment of new attachment following the treatment of a human buccal recession by means of a guided tissue regeneration procedure. J Periodontol 1993;64:387–391.
33. Pinheiro ALB, Gerbi MEMM, Limeira FA Jr, Ponzi EAC, Marques AMC, Carvalho CM, Santos RC, Oliveira PC, Noiá M, Ramalho LMP. Bone repair following bone grafting hydroxyapatite guided bone regeneration and infrared laser photobiomodulation: A histological study in a rodent model. Lasers Med Sci 2009;24:234–240.
34. Gerbi MEMM, Ponzi EAC, Ramalho LMP, Marques AMC, Carvalho CM, Oliveira RC, Oliveira PC, Noiá M, Pinheiro ALB. Infrared laser light further improves bone healing when associated with bone morphogenic proteins: An in vivo study in a rodent model. Photomed Laser Surg 2008;26:55–60.
35. Pinheiro ALB, Gerbi MEMM, Ponzi EAC, Ramalho LMP, Marques AMC, Carvalho CM, Oliveira RC, Oliveira PC, Noiá M. Infrared laser light further improves bone healing when associated with bone morphogenetic proteins and guided bone regeneration: An in vivo study in a rodent model. Photomed Laser Surg 2008;26:167–174.
36. Torres CS, Santos JN, Monteiro JSC, Amorim PG, Pinheiro ALB. Does the use of laser photobiomodulation, bone morphogenetic proteins, and guided bone regeneration improve the outcome of autologous bone grafts? An in vivo study in a rodent model. Photomed Laser Surg 2008;26:371–377.
37. Gerbi MEMM, Pinheiro ALB, Ramalho LMP. Effect of IR laser photobiomodulation on the repair of bone defects grafted with organic bovine bone. Lasers Med Sci 2008;23:313–317.
38. Lopes CB, Pacheco MT, Silveira L Jr, Duarte J, Cangussú MC, Pinheiro ALB. The effect of the association of NIR laser therapy BMPs, and guided bone regeneration on tibial fractures treated with wire osteosynthesis: Raman spectroscopy study. J Photochem Photobiol B 2007;89:125–130.
39. Lopes CB, Pinheiro ALB, Sathaiah S, Da Silva NS, Salgado MA. Infrared laser photobiomodulation (830 nm) on bone tissue around dental implants: A Raman spectroscopy and canning electronic microscopy study in rabbits. Photomed Laser Surg 2007;25:96–101.
40. Weber JBB, Pinheiro ALB, Oliveira MG, Oliveira FAM, Ramalho LMP. Laser therapy improves healing of bone defects submitted to autogenos bone graft. Photomed Laser Surg 2006;24:38–44.
41. Lopes CB, Pinheiro ALB, Sathaiah S, Duarte J, Martins MC. Infrared laser light reduces loading time of dental implants: A Raman spectroscopy study. Photomed Laser Surg 2005;23:27–31.
42. Gerbi MEMM, Pinheiro ALB, Marzola C, Limeira Junior FA, Ramalho LMP, Ponzi EAC, Soares AO, Carvalho LC, Lima HV, Gonçalves TO. Assessment of bone repair associated with the use of organic bovine bone and membrane irradiated at 830 nm. Photomed Laser Surg 2005;23:382–388.
43. Pinheiro ALB, Limeira Júnior FA, Gerbi MEMM. Effect of low level laser therapy on the repair of bone defects grafted with inorganic bovine bone. Braz Dent J 2003;14:177–181.
44. Pinheiro ALB, Limeira Júnior FA, Gerbi MEMM, Ramalho LMP, Marzola C, Ponzi EAC, Carvalho LCB, Lima HCAV, Gonçalves TO, Soares AO. Effect of 830-nm laser light on the repair of bone defects grafted with inorganic bovine bone and decalcified cortical osseous membrane. J Clin Laser Med Surg 2003;21:383–388.
45. Pinheiro ALB, Oliveira MAM, Martins PPM. Biomodulação da cicatrização óssea pós-implantar com o uso da laserterapia não-cirúrgica: Estudo por microscopia eletrônica de varredura. [Biomodulation of Peri-implant bone repair with lasertherapy: SEM study]. Rev FOUFBA 2001;22:12–19.

46. Silva N Jr, Pinheiro ALB, Oliveira MGA, Weissmann R, Ramalho LMP, Nicolau RA. Computadorized morphometric assessment of the effect of low-level laser therapy on bone repair: An experimental animal study. J Clin Laser Med Surg 2002;20:83–88.
47. Pinheiro ALB, Aciole GTS, Cangussú MCT, Pacheco MTT, Silveira L Jr. Effects of laser phototherapy on bone defects grafted with mineral trioxide aggregate, bone morphogenetic proteins, and guided bone regeneration: A Raman spectroscopic study. J Biomed Mater Res A 2010;95:1041–1047.
48. Mooney MP, Siegel MI. Animal models for bone tissue engineering of critical-sized defects (CSDs), bone pathologies, and orthopedic disease states. In: Hollinger JO, Einhorn TA, Doll BA, Sfeir C, editors. Bone Tissue Engineering. Boca Raton, FL: CRC Press;2005. p217–244.
49. Oliveira EA, Oliveira VGM, Pires JA, Barreto ALS, Ribeiro MAG, Pinheiro ALP, Marques AMC, Melo CM, Albuquerque Júnior RLC. Effect of low-level laser therapy and mineral trioxide aggregate on alveolar bone repair. Braz J Oral Sci 2008;27:1657–1661.
50. Liebschner MA. Biomechanical considerations of animal models used in tissue engineering of bone. Biomaterials 2004;25: 1697–1714.
51. Ebina H, Hatakeyama J, Onodera M, Honma T, Kamakura S, Shimauchi H, Sasano Y. Micro-CT analysis of alveolar bone healing using a rat experimental model of critical-size defects. Oral Dis 2009;15:273–280.
52. Young S, Kretlow JD, Nguyen C, Bashoura AG, Baggett LS, Jansen JA, Wong M, Mikos AG. Microcomputed tomography characterization of neovascularization in bone tissue engineering applications. Tissue Eng Part B Rev 2008;14:295–306.
53. Lee YL, Lee BS, Lin FH, Lin AY, Lan WH, Lin CP. Effects of physiological environments on the hydration behavior of mineral trioxide aggregate. Biomaterials 2004;25:787–793.
54. Romano PR, Caton JG, Puzas JE. The reversal line may be a key modulator of osteoblast function: Observations from an alveolar bone wound -healing model. J Periodontal Res 1997;32:143–147.
55. Palumbo C, Ferretti M, Ardizzoni A. Osteocyte-osteoclast morphological relationships and the putative role of osteocytes in bone remodeling. J Musculoskelet Neuronal Interact 2001;1:327–332.
56. Domon T, Suzuki R, Takata K, Yamazaki Y, Takahashi S, Yamamoto, Wakita M. The nature and function of mononuclear cells on the resorbed surfaces of bone in the reversal phase during remodeling. Ann Anat 2001;83:103–110.
57. Matsuda C, Takagi M, Hattori T, Wakitani S, Yoshida T. Differentiation of human bone marrow mesenchymal stem cells to chondrocytes for construction of three-dimensional cartilage tissue. Cytotechnology 2005;47:11–17.
58. Coneglian PZA. Avaliação do processo evolutivo do reparo ósseo frente ao sulfato de cálcio e à hidroxiapatita. Estudo microscópico em alvéolos dentários de ratos. [Assessment of the bone repair following the use of calcium sulphate or hidroyapatite. Light microscopic study on dental sockts of rats]. M.Sci Dissertation. Bauru (SP), School of Dentistry of Baurú, São Paulo University; 2007. 254 p.
59. Perinpanaygam H. Cellular response to mineral trioxide aggregate root-end filling materials. J Can Dent Assoc 2009;75:369–372.
60. Perez AL, Spears R, Gutman JL, Opperman LA. Osteoblasts and MG-63 osteosarcoma cells behave differently when in contact with ProRoot MTA and White MTA. Int Endod J 2000;36:564–570.
61. Camilleri J, Pitt Ford TR. Mineral trioxide aggregate: A review of the constituents and biological properties of the material. Int Endod J 2006;39:747–754.
62. Saidon J, He J, Zhu Q, Safavi K, Spangberg LSW. Cell and tissue reactions to mineral trioxide aggregate and Portland cement. Oral Surg Oral Med Oral Pathol Oral Radiol Endod 2003;95:483–489.